

Contents lists available at ScienceDirect

Physica C

journal homepage: www.elsevier.com/locate/physc



On the scaling law of some characteristic fields in $Y_{1-x}Pr_xBa_2Cu_3O_{7-\delta}$

V. Sandu ^{a,*}, Carmen C. Almasan ^b

ARTICLE INFO

Article history:
Received 29 June 2010
Received in revised form 24 November 2010
Accepted 20 December 2010
Available online 24 December 2010

Keywords: Second peak magnetization $Y_{1-x}Pr_xBa_2Cu_3O_{7-\delta}$ Anisotropy Pinning

ABSTRACT

We investigated the anisotropy dependence of the characteristic fields of the second peak magnetization, specifically, the onset field B_{on} and the peak field B_{sp} , in $Y_{1-x}P_{T_x}Ba_2Cu_3O_{7-\delta}$ single crystals. The empirical dependence arising from data analysis suggests a logarithmic dependence of both these fields on the anisotropy factor γ which disagrees with the universal scaling law $\gamma^2B=F(t)$ proposed previously. We attribute the faster decrease of the two fields at high anisotropy to the dramatic changes in the magnetic state of the system which starts to display a noticeable paramagnetic contribution at high Pr-doping, hence high anisotropy. The incipient phase separation could also reduce the elastic properties of the flux line lattice which determines onset of the second peak magnetization.

© 2010 Elsevier B.V. All rights reserved.

1. Introduction

The structure and phase transitions of the magnetic flux line system of rare earth (RE) cuprates REBa₂Cu₃O_{7-\delta} (RE-123 from here on) is directly related to the underlying crystal structure. Most rare earth elements can mutually substitute for each other in compounds like RE'_{1-x}RE''_x-123 keeping unaltered all physical properties [1] as well as the triple perovskite structure (pmmm space group). Moreover, there is a tight connection between the charge doping level and the lattice parameters for the same compound. The layered structure intensifies this dependence so that the interplane distances increases when the density of charge carrier decreases for all 123-compounds, no matter how the doping is achieved, either by partial substitution or by oxygenation. So, all systems become more and more anisotropic as the system is depleted of carriers mainly due to the decrease of the hopping integral on c-axis direction. For example, the anisotropy parameter γ , which is related to the ratio of the effective mass, is expected to increase continuously with decreasing the charge carrier concentration. Indeed, the in-plane effective mass m_{ab} was found to be almost insensitive to doping for both $La_{2-x}Sr_xCuO_4$ and $YBa_2Cu_3O_{7-\delta}$ [2] whereas the out-of-plane transport, hence, m_c is dependent on the interplane distance which increases with decreasing the charge density [3–5]. Data of Janossy et al. [6] confirm this anticipated behavior.

There is an exception when Pr substitute for RE. Although the triple perovskite structure is preserved for the whole range of concentrations *x*, the critical temperature and critical fields evolve

dramatically with increasing the content of Pr [7], specifically, the compound shows superconductivity for x < 0.55 while for higher Pr concentrations it is an insulating antiferromagnet. The anomalous behavior is attributed to the hybridization of the extended Pr4f orbitals with the adjacent O2p orbitals in superconducting Cu–O2 planes [8,9] which generates a localized Fehrenbacher–Rice (FR) band able to grab the free holes from the Zhang–Rice band [10] till the latter gets completely depleted.

It would be expected that the continuous depletion of charge carriers have similar effects with charge carrier depletion in other cuprates. Surprisingly, this is not the case of Pr-doped YBa₂Cu₃O₇. Despite the continuous increase of the c-axis lattice parameter [11,12] with increasing Pr, the anisotropy, as obtained from normal state transport measurements, has a peaked evolution as a function of doping with a maximum around x = 0.45 [13]. It can be the result of the interplay between rapid depletion of the charge carrier density, as well as the in-plane scattering effects on the magnetic perturbations created by the Pr ion [14].

It is obvious that the system of flux lines must be sensitive to the underlying atomic and magnetic structure. Actually, the phase diagram of the flux line system consists mainly of a quasiordered Bragg glass state with a power low decay of the correlation function of the vortex positions, a totally disordered vortex glass state with an exponential decay of the correlation function, and a vortex liquid. Several substates are present within each category depending on the circumstances. The transition between Bragg glass state and the vortex glass state is marked by a second magnetization peak [15–19]. Generally, the details of the peak are associated with the evolution, hence, the relationships, of the main energies involved in the characterization of the flux line system, i.e., the

^a National Institute of Materials Physics Bucharest, Magurele 077125, Romania

^b Department of Physics, Kent State University, Kent, OH 44242, USA

^{*} Corresponding author. E-mail address: vsandu@infim.ro (V. Sandu).

elastic E_{el} , pinning E_{pin} and thermal, k_BT , energies. In agreement with most models, the onset of the second magnetization peak occurs at the field B_{on} at which the pinning energy overcomes the elastic energy of the flux line lattice. Consequently, at B_{on} , the vortices start to break the long range order imposed by the elastic energy and occupy the most energetically comfortable positions. Above that field [20-24], dislocations proliferate and gradually the flux line system evolves toward an amorphous structure. Collective pinning theory provides the following dependences for the characteristic energies [25]: $E_{el}\varepsilon_0c_L^2a_0\gamma^{-1}$ and $E_{pin}=U_{dp}\left(\frac{L_0}{L_c}\right)^{\frac{1}{5}}$, where ε_0 is the energy scale of the vortex line, c_t^2 is the Lindemann factor, $a_0 \sim \left(\frac{\Phi_0}{R}\right)^{\frac{1}{2}}$ the lattice parameter of the flux line system, γ the anisotropy parameter, $U_{dp}=\left(rac{\delta_{dis}k_0 arepsilon^4}{\gamma^2}
ight)^{rac{1}{3}}$ is the depinning energy, $L_0=rac{2a_0}{\gamma}$, $L_c=\left(arepsilon_0^2 \xi^2 \gamma^{-4} \delta_{dis}^{-1}
ight)^{rac{1}{3}}$, ξ is the in-plane coherence length and δ_{dis} the isotropised disorder parameter. The dependence of the onset field B_{on} on the material parameters, anisotropy γ included, is obtained from the equilibrium condition between the elastic and pinning energies which gives:

$$B_{on} \sim \frac{c_L^5 \Phi_0 \varepsilon_0^2}{\delta_{dis} \xi^3 \gamma} \tag{1}$$

Consequently, more anisotropy leads to smaller onset field.

On the other side, the second magnetization peak B_{sp} is considered to define the crossover to the plastic dominated creep [26,27] where the plastic activation energy $U_{pl} = \varepsilon_0 a_0 \gamma^{-1}$ is of the order of the depinning energy U_{dp} . This condition gives:

$$B_{sp} \sim \frac{\Phi_0 \varepsilon_0^{\frac{4}{3}}}{\delta_{dis}^{\frac{2}{3}} \xi_0^{\frac{8}{3}} \gamma^{\frac{2}{3}}}$$
 (2)

Thus, neither B_{on} nor B_{sp} , as obtained by these conditions, follow the γ^{-2} -scaling reported by Kitazawa et al. [28] in the magnetic phase diagram of HTS. A similar claim is made in Ref. [29] based on the dynamic origin of the peak.

In this paper we show that in Pr-doped $YBa_2Cu_3O_7$ samples, the characteristic fields decrease slower than predict Eqs. (1) and (2) but both follow a similar logarithmic dependence as function on anisotropy.

2. Experimental details

In order to investigate the relation between anisotropy γ and the magnetic properties of superconductors, we used the dependence between charge carrier density and anisotropy. Consequently, we investigated a series of $Y_{1-x}Pr_xBa_2Cu_3O_{7-\delta}$ (x = 0.13, 0.34 and, 0.47) single crystals, in which Pr substitution for Y reduces the free charge density, hence, increases the distances between CuO₂ planes and reduces the c-axis charge mobility. The three single crystals for which data are presented here are platelets of size $1.25 \times 0.95 \times 0.12 \text{ mm}^3$, $0.75 \times 0.4 \times 0.1 \text{ mm}^3$, and $0.83 \times 0.47 \times 0.03 \text{ mm}^3$ with critical temperatures T_c of 82 K, 50 K, and, 34 K respectively. Details of the growth procedure are reported elsewhere [30]. For completeness, we also show data for x = 0 single crystals, taken from several Refs. [31–34]. We chose to use data from several references because it is well known the sensitivity of YBa₂Cu₃O_{7- δ} single crystals to the preparation conditions, environment and twinning, therefore the data are rather scattered but on average they support our statements. We also took the average anisotropy factor $\gamma = 6$ for the x = 0 samples.

Magnetic field H dependent magnetization M were performed at different temperatures T in the reduced temperature range T/T_c between 0.3 and 0.7 by using a MPMS (Quantum Design) supercon-

ducting quantum interference device magnetometer with the external magnetic field applied parallel to the c-axis of the single crystal. We used the persistent current mode with a scan length of 40 mm which guarantees excellent magnetic field homogeneity. The single crystals were cooled in zero field to the desired temperature and the whole M(H) loop was recorded in increasing and decreasing fields with H steps chosen to get the finest details in M(H). After performing a hysteresis loop at a given temperature, the sample was warmed up to $T >> T_c$ and zero-field-cooled to the next set temperature.

The in-plane ρ_{ab} and out-of-plane ρ_c resistivities and their temperature dependence were simultaneously measured in a PPMS (Quantum Design) system using a procedure described in the Ref. [35]. The critical temperature T_c was taken at the midpoint of the normal-superconductor transition. The anisotropy was determined as the ratio of out-of-plane and in-plane resistivities, $\gamma_\rho = (\rho_c | \rho_{ab})^{1/2}$ taken at the onset of the normal to superconducting transition. It was shown that this value is close to the anisotropy factor $\gamma = m_c | m_{ab}$ in the superconducting state as obtained from the temperature dependence of the melting field of the flux lines lattice [36] and the flow of the Josephson vortices [37] measurements. Therefore, we take $\gamma \cong \gamma_O$.

3. Results and discussion

Data for magnetization of three different Pr concentration, hence, for three different anisotropies, as measured for the same reduced temperature $t = T/T_c$ are shown in Fig. 1. The inset shows the increasing part of the anisotropy vs. Pr-doping. However, the anisotropy is not monotonous and decreases fast when the doping approaches the superconductivity limit x = 0.55. The data have been used to define the onset field B_{on} and second magnetization peak B_{sp} , as shown in the figure. The dependences of the two characteristic fields on anisotropy γ are presented in Fig. 2 for B_{on} and Fig. 3 for B_{sp} . Both fields obey similar law: $B_{on,sp}(\gamma,t) = B_0^{on,sp}(t) \log(\gamma_{\max}^{on,sp}/\gamma)$, where $B_0^{on,sp}(t)$ are temperature-dependent scaling fields, and $\gamma_{\max}^{on} \approx 33$, while $\gamma_{\max}^{sp} \approx 32.6$ It is interesting that the extrapolation toward $x_c = 0.55$ of the low doping part $(x \le 0.45$, i.e., beyond the peak) of γ vs. x curve provides $\gamma_c \equiv \gamma$ (x_c) = 32.8

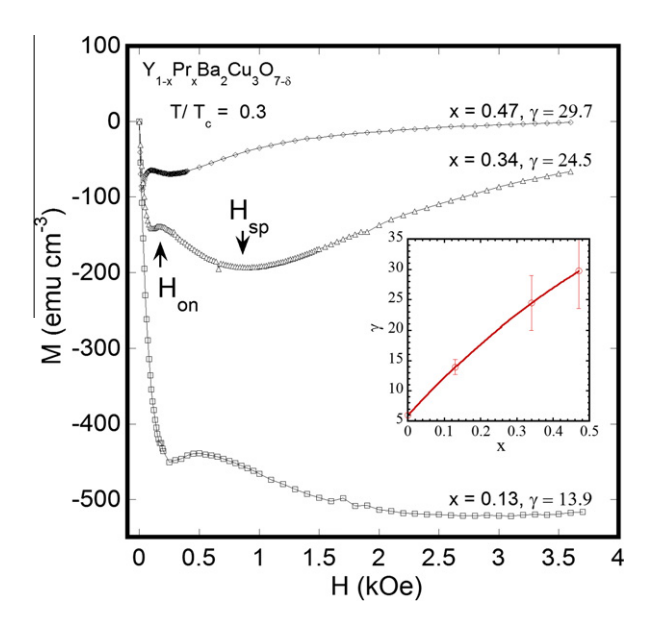


Fig. 1. Magnetization curves for $Y_{1-x}Pr_xBa_2Cu_3O_{7-\delta}$, x = 0.13, 0.34, and 0.47 single crystals, measured at the same reduced temperature $T/T_c = 0.3$. The arrows indicate the position of the onset H_{on} and second magnetization peak H_{sp} fields. Inset: the dependence of the anisotropy γ on the content of Pr.

Download English Version:

https://daneshyari.com/en/article/1818587

Download Persian Version:

https://daneshyari.com/article/1818587

<u>Daneshyari.com</u>